

Effect of Surface Morphology on the Ordered Water Layer at Room Temperature

Chunlei Wang,^{†,‡} Bo Zhou,^{†,‡} Peng Xiu,[§] and Haiping Fang^{*,†,||}

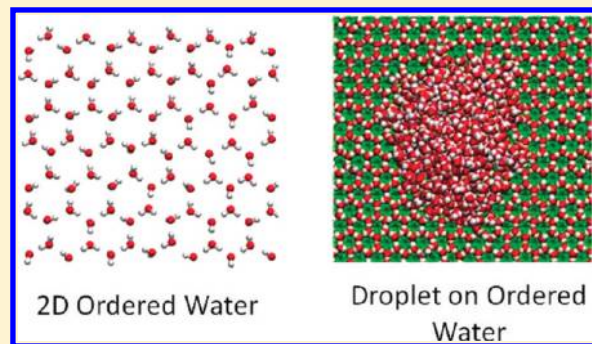
[†]Shanghai Institute of Applied Physics, Chinese Academy of Sciences, P.O. Box 800-204, Shanghai 201800, China

[‡]Graduate School of the Chinese Academy of Sciences, Beijing 100080, China

[§]Bio-X Lab, Department of Physics, Zhejiang University, Hangzhou, 310027, China

^{||}Theoretical Physics Center for Science Facilities, Chinese Academy of Sciences, 19(B) Yuquan Road, Beijing 100049, China

ABSTRACT: The behavior of water, particularly the first water layer residing on solid surfaces with various unit cell sizes and charge defects, is studied by molecular dynamics simulations at room temperature. We found that both the unit cell size and presence of defects greatly affected the configurations of the first water layer, specifically the structure and stability of the two-dimensional hydrogen-bond network within this layer. Consequently, the wetting behavior of water on the solid surface is significantly influenced. On certain wetted solid surfaces with water droplets distributed over the first water layer, the presence of defects at low ratios leads to partial disruption of the structure of the two-dimensional hydrogen-bond network within the first water layer and the existence of the irregular droplet profiles different from the conventional circular shapes. Due to the adsorption of the surface, the dwell time of the first water layer is extremely large and is about 1 order of magnitude larger than the rest of the water layers.



1. INTRODUCTION

The wetting behavior of surfaces,^{1–7} as characterized by hydrophobicity and hydrophilicity, has a fundamental bearing on various phenomena that arise in physics,^{8–13} chemistry,^{14–21} and biology.^{22–28} Hydrophobic effects have an important role in many important physiochemical processes, such as water permeation in membrane channels (aquaporins),^{29,30} superhydrophobic surface coating,^{14,17} and protein folding.^{31–33} Water confined on the nanometer scale, such as on the flat surface^{34–40} or nanopores,^{22,41–43} which exhibits novel ordered behavior, has recently gained special attention. This surface water is also particularly important in stabilizing structures of biological macromolecules and their functioning, especially in recognition at a specific sites.⁴⁴ Recently, it has been recognized that surface polarity has a crucial role in determining the behavior of water at hydrated interfaces. Giovambattista et al.⁴⁵ have shown that polar surfaces are macroscopically hydrophobic due to the limiting effect of polarity. They also showed that both topography and polarity of the surface act in concert with water and that surface hydrophobicity varied substantially according to surface geometry.⁴⁶ Zangi and Berne^{18,20} found that a larger charge density of ions in an aqueous medium unexpectedly strengthened hydrophobic rather than hydrophilic effects. Li et al.⁴⁷ have shown that the trichlorosilane molecule (CF₃(CF₂)_x(CH₂)_ySiCl₃, with -CF₃ terminating surfaces, is more hydrophobic than the hydrogenated -CH₃ surface, even though F atoms have larger partial charges than H atoms. They attributed this to the fact that van der Waals interactions, rather than electrostatic interactions, are the dominant interactions between surfaces and water.

Our previous simulations³⁷ have shown direct evidence of the unexpected phenomenon wherein, on a hexagonal polarity solid surface at room temperature, “water does not wet a water monolayer”. This phenomenon is attributed to the presence of an ordered structure of the water beneath the water droplet, the so-called “ordered water layer”. Very recently, Lützenkirchen et al.⁴⁸ have demonstrated their experimental results on a sapphire c-plane electrolyte interface in which this phenomenon can be quite favorably observed. In practice, it is not easy to fabricate the structure exactly as proposed in ref 37. On the one hand, due to competing mechanisms, certain materials may have different lattice structures even though these may be close to the structure proposed in ref 37. On the other hand, defects are in practice common in all fabricated nanomaterials.⁴⁹ Defects usually have an essential role in the properties of materials, such as electrical conductivity, optical absorption,⁵⁰ and wettability.⁵¹

Here, we present results from our study on the behavior of water, particularly the first water layer of surfaces having various unit cell sizes and defects, in molecular dynamics (MD) simulations at room temperature. We found that both the solid unit cell sizes and the presence of defects greatly affected the configurations of the first water layers, specifically the structure and stability of the two-dimensional hydrogen-bond network lying within the first water layer. On certain wetted solid surfaces with water droplets distributed over the first water layer, the presence

Received: September 9, 2010

Revised: January 5, 2011

Published: February 2, 2011

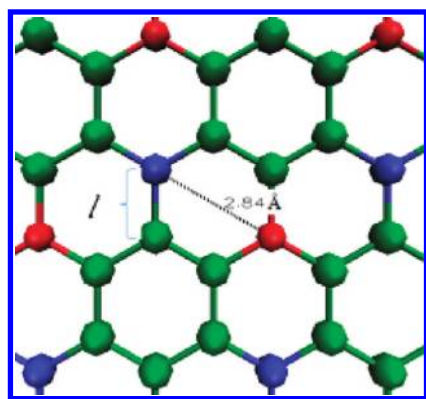


Figure 1. Hexagonal lattice of the solid surface showing charged pairs. Red and blue spheres represent solid atoms of opposite charge, and the green spheres represent neutral solid atoms.

of defects at low ratios leads to partial disruption of the structure of the two-dimensional hydrogen-bond network within the first water layer and the existence of irregular droplet profiles different from the conventional circular shapes. Due to the adsorption of the surface, the dwell time of the first water layer is extremely large and is about 1 order of magnitude larger than the rest of the water layers.

2. SYSTEMS AND METHODS

In our simulations, we configured a hexagonal solid lattice with 1664 solid atoms and nearest-neighbor bond length l as depicted in Figure 1a. Positive and negative charges of the same magnitude q are assigned to the atoms located diagonally in neighboring hexagons. We performed two series of simulations. In the first series of simulations, we have varied only the neighboring atom bond length l at 0.12, 0.13, 0.142, 0.15, and 0.16 nm while maintaining the charge q between 0.6e and 1.0e, with water molecules $N = 795, 838, 838, 838$, and 1043, respectively. The value of 0.142 nm corresponds to the C–C bond length in the graphene or graphite surface. Our simulations have shown that a slight change of this value (e.g., 0.14 nm) does not change the conclusion in this article. Initially, the water film completely covers the surface. Periodic boundary conditions were applied in all directions for all simulations of systems.

The second series of systems contained 1664 solid atoms, with $l = 0.142$ nm and $q = 1.0e$, and point defects generated by randomly eliminating a dipole pair from the hexagons on the solid surface, thus maintaining charge neutrality over the entire surface. The total number of point defects was set at 4, 20, 40, 80, and 120, corresponding to defect ratios of 1%, 5%, 10%, 20%, and 30%, respectively. The system contained 838 water molecules to form a film with a thickness of about 1.1 nm that completely covered the surface. The water slab was assumed to be in phase equilibrium with vapor at $T = 300$ K.

With a time step of 1.0 fs, the simulation time duration was 8 ns for fixed values of q and defect ratio, but only the last 4 ns of data was collected for analysis. The MD simulations were performed with Gromacs 3.3.1⁵² in an NVT ensemble at a temperature of 300 K. The solid atoms were characterized by the Lennard-Jones parameters $\epsilon_{ss} = 0.105$ kcal/mol and $\sigma_{ss} = 3.343$ Å, and the simple point charge (SPC/E) water model⁵³ was used. The particle-mesh Ewald method⁵⁴ with a real-space cutoff of 1 nm was used to treat long-range electrostatic interactions and a 10 Å cutoff was applied to all van der Waals interactions.

The water dwell time is characterized by the autocorrelation function

$$C(t) = \frac{\langle h(0)h(t) \rangle}{\langle h(0)h(0) \rangle} \quad (1)$$

where $h(t) = 1$ if the tagged water pair is in the same layer z at time 0 to time t and $h(t) = 0$ otherwise. We used double-exponential functions⁵⁵ to fit the data, with τ_{long} as the dwell time.

$$C(t) = A_{\text{long}} \exp(-t/\tau_{\text{long}}) + A_{\text{short}} \exp(-t/\tau_{\text{short}}) \quad (2)$$

3. RESULTS AND DISCUSSION

3.1. Effect of Solid Unit Cell Size on the Ordered Water Layer. For $l = 0.12$ and 0.16 nm with $0.6e \leq q \leq 1.0e$, we find that water completely wets the surface. In contrast, when $0.6e \leq q \leq 1.0e$ for $l = 0.142$ nm, and $0.8e \leq q \leq 1.0e$ for $l = 0.13$ and 0.15 nm, clear water droplets formed on the first water layer as shown in Figure 2a (see also ref 37). Moreover, as q increases over the interval, the contact angle of the droplet also increases (see Figure 2b). Our calculations indicate that the rest of the solid surfaces outside the droplet are covered by water molecules with an average thickness of 4.0 Å⁵⁶ (see Figure 2a), consistent with the existence of an experimentally observable monolayer. Thus, the water droplet is in fact above a water monolayer, which can be termed as “hydrophobic-like water”.

Due to the charges assigned to the atoms, water molecules are stably adsorbed on the surface. For a uniform measurement, we define the first water layer as those water molecules nearest to the solid surface within a thickness of 0.4 nm.³⁷ We have calculated the total interaction energy $E_{\text{solid-w}}$ (electrostatic plus van der Waals interactions) per water molecule associated with interactions between water molecules of the first water layer and atoms of the solid surface. The results are graphed in Figure 3a. It is found that this interaction energy increases as q increases. The strength of the interaction accounts for the stability of the water layer formed by the molecules adsorbed on the solid surface and partially is responsible for the formation of the ordered water layer (see below). However, this interaction does not explain the emergence of the droplet on the surface (see Figure 3b). It should be noted that the total interaction energy $E_{\text{solid-w}}$ per water molecule associated with interactions between water molecules of the first water layer and atoms of the solid surface is the partial basis of the ordered structure of the water monolayer and is the partial origin of the hydrophobicity of the ordered water monolayer.

To further understand the stable droplet standing on the highly polar surface, we have studied the first water layer configuration near the solid surface for l between 0.12 and 0.16 nm. At $l = 0.13, 0.142$, and 0.15 nm and a relatively large q , it is very interesting to find that a 2D-ordered hexagonal water monolayer beneath the water droplet has formed on the solid surface. For $l = 0.142$ nm and $q = 1.0e$, Figure 4a displays a snapshot of the water structure and Figure 4b displays two typical configurations of binding states for water molecules.

Herein, we introduce two angle parameters, φ and Ψ , to be defined below, to describe the ordered water configuration in the first water layer. First, this ordered hexagonal structure is confirmed by the probability distribution of φ , where φ is the angle formed between the projection onto the x – y plane of a water dipole and a crystallographic direction. We show a typical distribution given $q = 1.0e$ in Figure 5a, where there is a clear

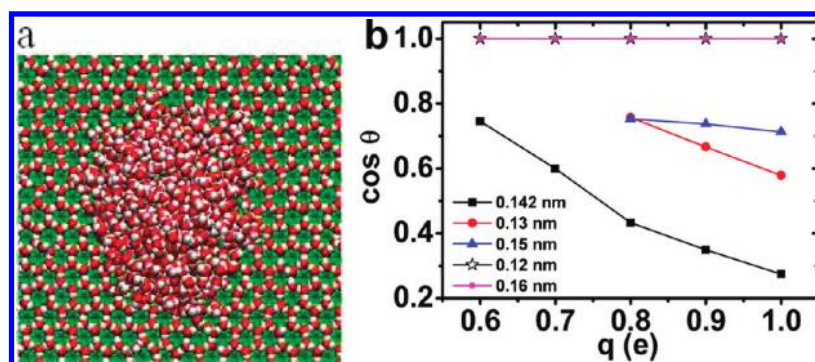


Figure 2. (a) Simulation snapshot of water molecules on a solid surface when $q = 1.0e$ and $l = 0.142$ nm. (b) Contact angle vs q for $l = 0.12, 0.13, 0.142, 0.15$, and 0.16 nm.

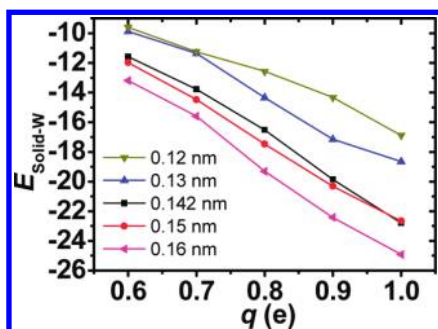


Figure 3. Total interaction energy per water molecule associated with interactions with solid atoms and water molecules in the first water layer vs q for various l .

orientation preference of the water dipole with three peaks at $\varphi = 0^\circ, 120^\circ$, and 240° . These three peaks perfectly correspond to the hexagonal 2D hydrogen-bond networks in Figure 4b. In contrast, the distributions with $l = 0.12$ and 0.16 nm show much lower peaks than the others ($l = 0.13, 0.142$, and 0.15 nm) despite the large charge value of $q = 1.0e$. Second, Figure 5b shows the normalized probability distribution of the dipole orientation Ψ of the water molecules of the first water layer when $q = 1.0e$, where Ψ is the angle between a water dipole and the z axis. It is clear that there are two peaks corresponding to the two binding states of water, denoted as states 1 and 2, respectively, and depicted in Figure 4b. This angle Ψ also reflects ordered configurations of the binding water molecules. The water molecule in state 1 has both -OHs pointing to neighboring water molecules, forming two hydrogen bonds. The water molecule in state 2 has one -OH pointing to the surface plane on account of the electrostatic interactions and the other -OH pointing to another water molecule, forming just one hydrogen bond. Note that the hexagonal solid/charged atom substrate here ensures that every water molecule has three neighboring water molecules and tends to form three hydrogen bonds. This structure with two binding states is quite similar to the H-down configuration of the first water layer binding on Pt(111) surfaces at ~ 135 K.^{34,35} Note also that when $l = 0.12$ and 0.16 nm, the peaks are lower than when $l = 0.13, 0.14$, and 0.15 nm despite the large charge value $q = 1.0e$.

Furthermore, this specific ordered water configuration could induce a tendency toward hydrogen-bond saturation for every water molecule. We have calculated the hydrogen-bond number for water molecules in this monolayer beneath the droplet. With the specification that a hydrogen bond between water molecules satisfies the simultaneous conditions that the O—O distance

must be less than 3.5 \AA and the angle $\text{O—H} \cdots \text{O}$ is less than 30° , then the hydrogen bond number is found to be ~ 2.6 . Alternatively, if we specify that the angle $\text{O—H} \cdots \text{O}$ must be less than 35° , then the hydrogen-bond number increases to ~ 2.8 . Both of these values are relatively close to 3. Consider the fact that for each water molecule that can form a H-bond with other water molecules, approximately one site is occupied on account of the electrostatic interaction with the surface charges. Thus, the total number of hydrogen bonds formed by a water molecule in the monolayer beneath the droplet approaches 4, which represent the maximum capacity of hydrogen bonds that a water molecule can form. Clearly, such a saturation configuration results in a form of hydrogen-bond quenching between water molecules in this monolayer and water molecules above. The net effect is that the probability of forming hydrogen bonds between water molecules in the first water layer and droplet above will greatly decreases as q increases, and the corresponding electrostatic interactions $E_{\text{M-D}}$ between them will decrease likewise. A typical result for $l = 0.142$ nm is shown in Figure 6. Unexpectedly, the electrostatic interactions between water molecules of the monolayer and the first water layer significantly decrease by ~ 10 kJ/mol as q increases from $0.6e$ to $1.0e$. This is consistent with the fact that the average number of hydrogen bonds formed by each water molecule in the first layer with water molecules above decreases by ~ 0.3 . We emphasize that this decrease in the hydrogen-bond number and electrostatic interaction is the physical origin of the stable liquid water droplet on the first layer, which shows the first water layer becomes hydrophobic-like.

Our simulation results have shown that when $0.13 \text{ nm} \leq l \leq 0.15 \text{ nm}$, the water droplet still emerges above the first water layer as shown in Figure 3b. During the interval, when $l = 0.142$ nm, the maximum contact angle of the water droplet appears. Why does the maximum point appear at $l = 0.142$ nm? To address this issue, we have performed simulations with 416 water molecules adsorbed on this surface with l ranging from 0.12 to 0.16 nm, and the surface covered with a full layer. Because the adsorption on the solid surface is very stable, we are able to calculate the electrostatic interaction energies $E_{\text{W-W}}$ for each neighboring water—water pair. This interaction is able to reflect the stability of the ordered hydrogen-bond network of the first water layer. We show a typical result for $q = 1.0e$ in Table 1, and remarkably, the largest $E_{\text{W-W}}$ value corresponds to the largest contact angle. When $q = 1.0e$, energies $E_{\text{W-W}}$ for various l values are quite different and the maximum interaction energy is -27.3 kJ/mol at $l = 0.142$ nm. This value is larger than -26.7 kJ/mol for $l = 0.13$ nm, $q = 1.0e$ and -23.5 kJ/mol for $l = 0.15$ nm, $q = 1.0e$. This

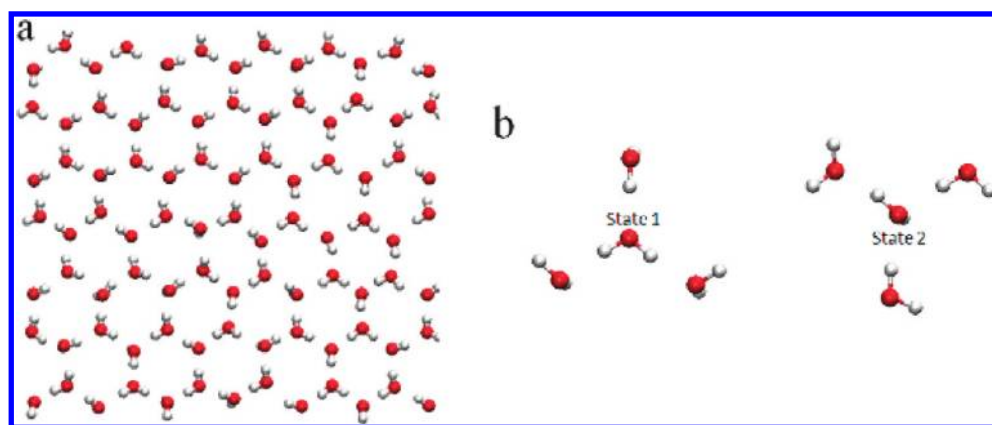


Figure 4. (a) Ordered water structure of the first water layer on the hexagonal solid surface when $l = 0.142$ nm and $q = 1.0e$. (b) Two typical configurations of binding states for water molecules on this solid surface, when $l = 0.142$ nm and $q = 1.0e$.

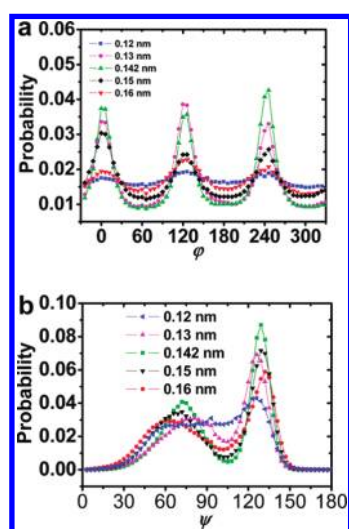


Figure 5. (a) Angular probability distribution for angle ϕ between the x - y plane projection of one water molecule dipole orientation and a crystallographic direction at hexagonal solid surface. (b) Probability distribution of the dipole orientation Ψ of water molecules in the first water layer near the solid surface, where Ψ is the angle between the water molecule dipole orientation and the z axis. Both panels were obtained with charge magnitude $q = 1.0e$.

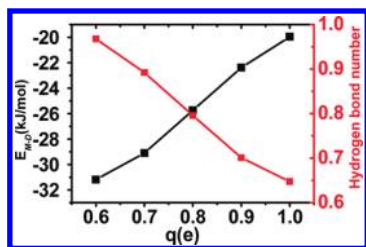


Figure 6. Average interaction energy E_{M-D} between a single water molecule in the first water layer with others in the same layer and with those above (black square), and the corresponding hydrogen-bond number (red square), for $l = 0.142$ nm.

energy difference could explain why the maximum contact angle for water droplets appears at $l = 0.142$ nm. The most stable hydrogen-bond network formed in between the water monolayer molecules at $l = 0.142$ nm could lead to the result that water

Table 1. Parameters of Length, Contact Angle, and Electrostatic Interaction Energies for Each Neighboring Water–Water Pair and the Number of Hydrogen Bonds That Form between the Monolayer and the Water Molecules, When $q = 1.0e$

l (nm)	0.12	0.13	0.142	0.15	0.16
contact angle (deg)	0 ^a	60.4	74.0	44.5	0 ^a
E_{W-W} (kJ/mol)	−19.1	−26.7	−27.3	−23.6	−21.3
H-bonds	0.9	0.72	0.65	0.79	0.89

^a For simplicity, when we cannot observe a clear droplet, the contact angle is set to 0.

molecules in the monolayer may prefer to form hydrogen bonds with water molecules in the same monolayer, rather than forming hydrogen bonds between the monolayer and the water molecules above. For each water molecule in the monolayer beneath the droplet, we have calculated the number of hydrogen bonds that form between the monolayer and the water molecules above for various l values with $q = 1.0e$. The results are also listed in Table 1. When $l = 0.12$ and 0.16 nm, with $q = 1.0e$, the average number of hydrogen bonds between the first water layer and the water above is ~ 0.9 and ~ 0.89 , respectively, both of which are larger than the alternatives: (i) ~ 0.65 when $l = 0.142$ nm, (ii) ~ 0.72 when $l = 0.13$ nm, and (iii) ~ 0.79 when $l = 0.15$ nm, all with $q = 1.0e$. This is thus consistent with the fact that the contact angle when $l = 0.142$ nm and $q = 1.0e$ is larger than for other l values. Thus, when $l = 0.142$ nm, the number of hydrogen bonds formed between water monolayer and water above is at a minimum and the water monolayer is at its most hydrophobic; namely, the contact angle is at its largest.

3.2. Effect of Point Defects on the Ordered Water Layer.

When $0.6e \leq q \leq 1.0e$ with $l = 0.142$ nm, a water droplet would appear on the water monolayer;³³ see also Figure 2b. The well-defined charge distribution of the solid surface should be responsible for this phenomenon. In this section, we will focus on the effect of point defects on this novel wetting behavior. We have systematically varied the defect ratio from 1% to 30% for $q = 1.0e$ and $l = 0.142$ nm. The snapshots of simulations are shown in Figure 7a–d. It is found that the first water layer on the solid surface is gradually covered by the water molecules of the irregularly shaped droplet as the defect ratio increases. As a comparison, the behavior of water molecules for $q = 1.0e$ without any defects is shown in Figure 2b.

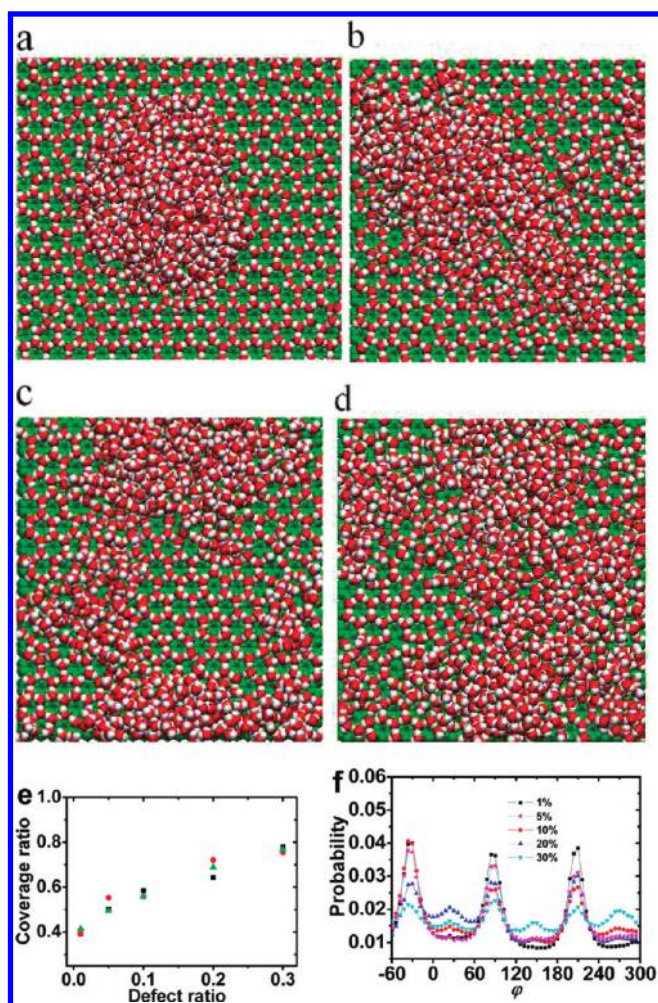


Figure 7. Simulation snapshots of water molecules on a solid surface when $q = 1.0e$ and $l = 0.142$ nm, at various defect ratios: (a) 1%, (b) 10%, (c) 20%, and (d) 30%. Irregular-shaped water droplets appear over the first water layer on the solid surface over the entire range of defect ratios. (e) Relationship between the defect ratio and the coverage ratio, which demonstrates the hydrophobicity of the first water layer, when $q = 1.0e$ and $l = 0.142$ nm. (f) The ordered configuration of the first water layer disappears for various defect ratios.

It is clear that the contact angle is not suitable to characterize the hydrophobicity of a surface with defects, as the structure of the water droplet is irregular. Therefore, we define a parameter, called the coverage ratio, to characterize the behavior of a water droplet on a defect-covered surface. This coverage ratio is defined as the ratio of the number of water molecules that cover the first water layer to the number of water molecules in the first water layer. In practice, we calculated the number of water molecules in the first water layer with a thickness of 0.4 nm from the solid surface and the number of second-layer water molecules above the first water layer with a thickness of 0.4 nm. To provide convincing support for our notion, we took three independent systems with various random defect distributions for every defect ratio. As shown in Figure 7e, the coverage ratio increases as the defect ratio increases, indicating that the hydrophobicity of the first water layer decreases. This can be attributed to the fact that the presence of solid defects obviously affects and disrupts the stability of the ordered first water layer. As shown in Figure 7f, the ordered configuration of the first water layer disappears when the

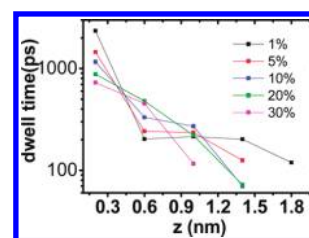


Figure 8. Average dwell time of the water molecules in 0.4 nm thickness layers vs different distances z from the solid surface at various defect ratios on solid surface.

defect ratio is high. Thus the results are that as the defect ratio increases, the coverage ratio increases, which clearly demonstrates that the first water layer becomes less hydrophobic compared with a surface with no solid defects. We also find that, for various defect distributions at the same defect ratios, the effect of point defects on the coverage ratio is quite reliable.

We have calculated the average dwell time for the water molecules depending on the value of the z coordinates of the water molecules near the solid surface with various defect ratios. Here the thickness of the water layer bin is 0.4 nm. The results are shown in Figure 8. Due to the adsorption of the surface, the dwell time of the first water layer is extremely large and is about 1 order of magnitude larger than the rest of the water layers. The extremely large dwell times of water molecules may indicate a remarkably drop of kinetic energy due to unilateral spatial restriction by the solid surface. This is equivalent with less thermal movements (fluctuations), which may indicate an increase in density, as others reported.⁵⁷ This increase of the density may have quite important indications even in cell biology.⁵⁸ As the defect ratios increase, the adsorption effect of the solid surface decreases, which makes the dwell time of the first water layer decrease as shown in Figure 8. As for the second layer, the dwell time almost increases as the defect ratios increase. It may be attributed that the first water layer would influence the second layer through forming more hydrogen bonds as the defect ratios increase. Clearly, the solid defects obviously affect and disrupt the stability of the ordered first water layer, which is also favorable with the previous analysis.

4. CONCLUSIONS

We have studied the behavior of water, particularly the first water layer, on surfaces of various unit cell sizes and defects in molecular dynamics simulations at room temperature. We found that both cell size and the presence of defects greatly affect the configuration of the first water layer, specifically the structure and stability of the two-dimensional hydrogen-bond network within the first water layer. On certain wetted solid surfaces with water droplets distributed over the first water layer, the presence of defects at low ratios leads to partial disruption of the structure of the two-dimensional hydrogen-bond network within the first water layer and the existence of the irregular droplet profiles different from the conventional circular shapes. Koga et al.⁵⁹ studied the behavior of a thin film of water confined to a slit nanopore with smooth walls. The ice crystal of bilayer consisting of rows of distorted hexagons, the bilayer ice has a feature that is common to all known ice polymorphs: every water molecule is hydrogen-bonded to its four neighbors. However, this confinement bilayer ice is distinctly different from our work with an in-plane hexagonal monolayer with four potential hydrogen-bond sites

occupied by its three neighboring water molecules and one by the charged surface. Zangi and Mark⁶⁰ have found ordering layer induced by the confinement and the ice monolayer has an in-plane rhombic symmetry with respect to the positions of the oxygen atoms. This out-of-plane displacement, together with the rhombic arrangement of the nearest neighbors, is also different from our in-plane hexagonal ordered water monolayer.

Our work provides a better understanding of the novel wetting behavior of the first water layer on a surface at room temperature. It is clearly shown that water molecules on the charge-modified hydrophilic surfaces are necessarily more bound to the surface with higher dwell times and higher ordering configurations. In particular, our work would be useful in the actual fabrication of this novel material,⁴⁸ which may have potential applications in water treatment and self-cleaning of surfaces. It is expected that this study may also expand our knowledge on the relationship between surface geometry and surface wetting behavior.

AUTHOR INFORMATION

Corresponding Author

*E-mail: fanghaiping@sinap.ac.cn.

ACKNOWLEDGMENT

We thank Drs. Wenpeng Qi and Yusong Tu and the anonymous referees for their important suggestions. This work was supported by grants from Chinese Academy of Sciences, the National Science Foundation of China under Grant 10825520, the National Basic Research Program of China under Grant 2007CB936000, Shanghai Leading Academic Discipline Project (B111), and Shanghai Supercomputer Center of China.

REFERENCES

- Thiel, P. A.; Madey, T. E. *Surf. Sci. Rep.* **1987**, *7*, 211.
- Chandler, D. *Nature* **2005**, *437*, 640.
- Ashbaugh, H. S.; Pratt, L. R. *Rev. Mod. Phys.* **2006**, *78*, 159.
- Ewing, G. E. *Chem. Rev.* **2006**, *106*, 1511.
- Raschke, T. M. *Curr. Opin. Struct. Biol.* **2006**, *16*, 152.
- Verdaguer, A.; Sacha, G. M.; Bluhm, H.; Salmeron, M. *Chem. Rev.* **2006**, *106*, 1478.
- Ball, P. *Chem. Rev.* **2008**, *108*, 74.
- Hummer, G.; Garde, S. *Phys. Rev. Lett.* **1998**, *80*, 4193.
- Schneemilch, M.; Quirke, N.; Henderson, J. R. *J. Chem. Phys.* **2004**, *120*, 2901.
- Meng, S.; Zhang, Z. Y.; Kaxiras, E. *Phys. Rev. Lett.* **2006**, *97*, No. 036107.
- Li, J. Y.; Gong, X. J.; Lu, H. J.; Li, D.; Fang, H. P.; Zhou, R. H. *Proc. Natl. Acad. Sci. U.S.A.* **2007**, *104*, 3687.
- Yuan, Q. Z.; Zhao, Y. P. *Phys. Rev. Lett.* **2010**, *104*, No. 246101.
- Hu, G. H.; Xu, A. J.; Xu, Z.; Zhou, Z. W. *Phys. Fluids* **2008**, *20*, No. 102101.
- Genzer, J.; Efimenko, K. *Science* **2000**, *290*, 2130.
- Scatena, L. F.; Brown, M. G.; Richmond, G. L. *Science* **2001**, *292*, 908.
- Meng, S.; Xu, L. F.; Wang, E. G.; Gao, S. W. *Phys. Rev. Lett.* **2002**, *89*, No. 176104.
- Erbil, H. Y.; Demirel, A. L.; Avci, Y.; Mert, O. *Science* **2003**, *299*, 1377.
- Zangi, R.; Berne, B. J. *J. Phys. Chem. B* **2006**, *110*, 22736.
- Michaelides, A.; Morgenstern, K. *Nat. Mater.* **2007**, *6*, 597.
- Zangi, R.; Hagen, M.; Berne, B. J. *J. Am. Chem. Soc.* **2007**, *129*, 4678.
- Xiu, P.; Zhou, B.; Qi, W. P.; Lu, H. J.; Tu, Y. S.; Fang, H. P. *J. Am. Chem. Soc.* **2009**, *131*, 2840.
- Hummer, G.; Rasaiah, J. C.; Noworyta, J. P. *Nature* **2001**, *414*, 188.
- Pal, S. K.; Zewail, A. H. *Chem. Rev.* **2004**, *104*, 2099.
- Zhou, R. H.; Huang, X. H.; Margulis, C. J.; Berne, B. J. *Science* **2004**, *305*, 1605.
- Cicero, G.; Grossman, J. C.; Schwegler, E.; Gygi, F.; Galli, G. J. *Am. Chem. Soc.* **2008**, *130*, 1871.
- Fawzi, N. L.; Phillips, A. H.; Ruscio, J. Z.; Doucleff, M.; Wemmer, D. E.; Head-Gordon, T. *J. Am. Chem. Soc.* **2008**, *130*, 6145.
- Giovambattista, N.; Lopez, C. F.; Rossky, P. J.; Debenedetti, P. G. *Proc. Natl. Acad. Sci. U.S.A.* **2008**, *105*, 2274.
- Serr, A.; Horinek, D.; Netz, R. R. *J. Am. Chem. Soc.* **2008**, *130*, 12408.
- de Groot, B. L.; Grubmüller, H. *Science* **2001**, *294*, 2353.
- Beckstein, O.; Sansom, M. S. P. *Proc. Natl. Acad. Sci. U.S.A.* **2003**, *100*, 7063.
- Brooks, C. L.; Gruebele, M.; Onuchic, J. N.; Wolynes, P. G. *Proc. Natl. Acad. Sci. U.S.A.* **1998**, *95*, 11037.
- Dobson, C. M.; Sali, A.; Karplus, M. *Angew. Chem., Int. Ed.* **1998**, *37*, 868.
- Brooks, C. L.; Onuchic, J. N.; Wales, D. J. *Science* **2001**, *293*, 612.
- Ogasawara, H.; Brena, B.; Nordlund, D.; Nyberg, M.; Pelmenchikov, A.; Pettersson, L. G. M.; Nilsson, A. *Phys. Rev. Lett.* **2002**, *89*, No. 276102.
- Kimmel, G. A.; Petrik, N. G.; Dohnalek, Z.; Kay, B. D. *Phys. Rev. Lett.* **2005**, *95*, No. 166102.
- Sommer, A. P.; Zhu, D.; Bruhne, K. *Cryst. Growth Des.* **2007**, *7*, 2298.
- Wang, C. L.; Lu, H. J.; Wang, Z. G.; Xiu, P.; Zhou, B.; Zuo, G. H.; Wan, R. Z.; Hu, J. Z.; Fang, H. P. *Phys. Rev. Lett.* **2009**, *103*, No. 137801.
- Zuo, G. H.; Hu, J.; Fang, H. P. *Phys. Rev. E* **2009**, *79*, No. 031925.
- Sommer, A. P.; Zhu, D.; Foersterling, H. D.; Scharnweber, T.; Welle, A. *Cryst. Growth Des.* **2008**, *8*, 2620.
- Sommer, A. P.; Zhu, D.; Mester, A. R.; Foersterling, H. D.; Gente, M.; Caron, A.; Fecht, H. J. *Cryst. Growth Des.* **2009**, *9*, 3852.
- Tu, Y. S.; Xiu, P.; Wan, R. Z.; Hu, J.; Zhou, R. H.; Fang, H. P. *Proc. Natl. Acad. Sci. U.S.A.* **2009**, *106*, 18120.
- Wan, R. Z.; Lu, H. J.; Li, J. Y.; Bao, J. D.; Hu, J.; Fang, H. P. *Phys. Chem. Chem. Phys.* **2009**, *11*, 9898.
- Tu, Y. S.; Zhou, R. H.; Fang, H. P. *Nanoscale* **2010**, *2*, 1976.
- Zhou, Y. Q.; Karplus, M. *Nature* **1999**, *401*, 400.
- Giovambattista, N.; Debenedetti, P. G.; Rossky, P. J. *J. Phys. Chem. B* **2007**, *111*, 9581.
- Giovambattista, N.; Debenedetti, P. G.; Rossky, P. J. *Proc. Natl. Acad. Sci. U.S.A.* **2009**, *106*, 15181.
- Li, X.; Li, J. Y.; Eleftheriou, M.; Zhou, R. H. *J. Am. Chem. Soc.* **2006**, *128*, 12439.
- Lutzenkirchen, J.; Zimmermann, R.; Preocanin, T.; Filby, A.; Kupcik, T.; Kuttner, D.; Abdelmonem, A.; Schild, D.; Rabung, T.; Plaschke, M.; Brandenstein, F.; Werner, C.; Geckeis, H. *Adv. Colloid Interface Sci.* **2010**, *157*, 61.
- Hashimoto, A.; Suenaga, K.; Gloter, A.; Urita, K.; Iijima, S. *Nature* **2004**, *430*, 870.
- Queisser, H. J.; Haller, E. E. *Science* **1998**, *281*, 945.
- Dimeglio, J. M. *Europhys. Lett.* **1992**, *17*, 607.
- Lindahl, E.; Hess, B.; van der Spoel, D. *J. Mol. Model.* **2001**, *7*, 306.
- Berendsen, H. J. C.; Grigera, J. R.; Straatsma, T. P. *J. Phys. Chem.* **1987**, *91*, 6269.
- Darden, T.; York, D.; Pedersen, L. J. *Chem. Phys.* **1993**, *98*, 10089.
- Makarov, V. A.; Andrews, B. K.; Smith, P. E.; Pettitt, B. M. *Biophys. J.* **2000**, *79*, 2966.

- (56) Miranda, P. B.; Xu, L.; Shen, Y. R.; Salmeron, M. *Phys. Rev. Lett.* **1998**, *81*, 5876.
- (57) Sommer, A. P.; Pavlath, A. E. *Cryst. Growth Des.* **2007**, *7*, 18.
- (58) Sommer, A. P.; Zhu, D.; Scharnweber, T. *J. Controlled Release* **2010**, *148*, 131.
- (59) Koga, K.; Zeng, X. C.; Tanaka, H. *Phys. Rev. Lett.* **1997**, *79*, 5262.
- (60) Zangi, R.; Mark, A. E. *Phys. Rev. Lett.* **2003**, *91*, No. 025502.